J Mater Sci: Mater Med (2007) 18:807–817
DOI 10.1007/s10856-006-0002-4

Wettability modification and the subsequent manipulation of protein adsorption on a Ti6Al4V alloy by means of CO_2 laser surface treatment

L. Hao · J. Lawrence

Received: 7 June 2005 / Accepted: 8 December 2005 / Published online: 14 December 2006

Abstract Improvements in the wettability of the Ti6Al4V alloy following CO_2 laser treatment were identified as being due mainly to the increase in surface roughness, surface oxygen content and surface energy of the material. Untreated and mechanically roughened samples had higher amounts of adsorbed albumin and lower amounts of adsorbed fibronectin than CO_2 laser treated samples. Moreover, as the wettability of the Ti6Al4V alloy increased the adsorbed amounts of fibronectin increased, while the adsorbed amounts of albumin decreased—indicating the controllability of the CO_2 laser process. From this finding it is possible to assert that the wettability of the Ti6Al4V alloy was the prime influence on the observed changes in in vitro protein adsorption. Further, the noted considerable change in the polar component of surface energy, γ_{sv}^{p}, on the protein adsorption implied that the protein adsorption on the Ti6Al4V alloy was probably due to the polar and chemical interactions. This work has demonstrated that CO_2 laser radiation could be a suitable means to modify the wettability of the Ti6Al4V alloy and thereby manipulate protein adsorption and consequently render the material more bone cell responsive.

L. Hao (✉)
School of Engineering, Computer Science and Mathematics, University of Exeter, Exeter EX4 4QF, UK
e-mail: l.hao@lboro.ac.uk

J. Lawrence
Wolfson School of Mechanical and Manufacturing Engineering, Rapid Manufacturing Research Group, Loughborough University, Leicestershire LE11 3TU, UK

1 Introduction

Titanium and some of its alloys are now the dominant biomaterials on account of their good biocompatibility, load-bearing capacity and wear resistance. Commercially pure titanium (cp Ti) implants are alloplastic materials used as the foundation for replacing teeth in dentistry and are also used for orthopaedics; however, this interaction does not involve a chemical bond with bone. The lack of ability to bond chemically may lead to slow fixation of cp Ti dental implants and to their gradual loosening over a long period [1].

During the past decades, substantial progress has been made in understating the mechanisms of protein adsorption [2–4]. Extensive effect has been made to understand the cell-material interface and especially the protein-medicated events. The process of cell adhesion involves adsorption of proteins to the substrate, contact and attachment of cells, followed by spreading on the substrate [5]. The surface chemistry of the material surface and the adsorption of individual proteins can influence cell attachment [6, 7] and the hydrophilicity of the substrate [8] and surface energy of the material can influence which proteins are adsorbed [9]. Numerous research groups have studied the interactions of different types of cultured cells with biomaterials with different wettability to correlate the relationship between surface wettability and blood-, cell-, or tissue-compatibility for polymeric materials [10–12]. Furthermore, the surface wettability has a significant influence on the friction behaviour of a tribological system and gives an indication of its biotolerance: in a first approximation, the more wettable the material is, the better the human body tolerates it [13]. Proteins bind rapidly to biomaterial

surfaces and this adsorbed protein layer influences cell attachment and may subsequently affect tissue integration [14]. Compositional differences in the adsorbed protein layer and the conformation or orientation of the adsorbed protein on different substrates may be important in cell interactions [6].

Compared with established techniques for enhancing the biocompatibility of biomaterials, laser surface processing offers greater degrees of effectiveness, higher controllability and more rapid processing times. Because of these benefits, an increasing amount of work has been conducted into the use of lasers such a purpose. Morzadeh et al. used a pulsed CO_2 laser to graft a polymer [15] and a rubber [16]. The results showed a marked reduction of the platelet adhesion and aggregation for the modified polymer surface and cell attachment with greater degree of spreading and flattening on the unmodified rubber surface. L929 fibroblast cells attached and proliferated extensively on the CO_2 and KrF laser treated films [17] in comparison with the unmodified PET, with surface morphology and wettability being found to affect cell adhesion and spreading. More recently, Hao and Lawrence found CO_2 laser treatment generated surface properties on magnesia partially stabilised zirconia (MgO-PSZ) that resulted in bone apatite apatite formation in stimulated body fluid [18], favourable albumin [19] and fibronectin adsorption [20], better human fibroblast response [21] and better human osteoblast cell adhesion [22] and functions [23]. In addition, Hao and Lawrence demonstrated that the surface treatment using high diode power laser brought about higher wettability and improved stimulated physiological liquid response on bio-grade 316 LS stainless steel [24] and better osteoblast cell adhesion and proliferation on Ti6Al4V alloy [25]. Yet no work has so far investigated the use of CO_2 laser radiation to alter protein adsorption on any bio-grade metals.

This study investigates the fundamental interactions between human serum albumin and human plasma fibronectin proteins with a Ti6Al4V alloy following CO_2 laser surface treatment. The effects of CO_2 laser surface treatment on the wettability and protein adsorption of the Ti6Al4V alloy were compared with a mechanical roughening method—the conventional technique for improving osseointegration. Changes in the surface properties of the Ti6Al4V alloy occasioned by the CO_2 laser treatment were characterised and the wettability of the untreated, mechanically roughened and the CO_2 laser treated specimens were quantified. The thickness of the adsorbed human serum albumin and human plasma fibronectin layer on the untreated and CO_2 laser treated material were measured using ellipsometry and the relationship between the surface properties of the Ti6Al4V alloy in various states and protein adsorption were analysed and discussed.

2 Experimental procedures

2.1 Material details

The as-received Ti6Al4V alloy (ground annealed) used in this study was obtained in the form of a round bar with a diameter of 28.5 mm (Carpenter, Inc.). The composition of the Ti6Al4V alloy was: 88.3–90.8 wt% Ti, 5.5–6.5 wt% Al, 3.5–4.5 wt% V, <0.08 wt% C, 0.0125 wt% H, <0.25 wt% Fe, <0.05 wt% N and <0.13 wt% O. For experimental purposes, the round bar was divided into 16 sections each of 3 mm thickness with a cutting machine (Miniton; Struers, GmbH) using a diamond rimmed blade. The 16 divided sections were then separated into four groups of four samples each, with the groups being: untreated, mechanically roughened and CO_2 laser treated at two different laser power densities. For the mechanically roughened group, the samples were roughened by evenly abrading the entire surface of the sample with grinding paper (180 grit SiC). This was achieved by applying the grinding paper to the surface of the sample with moderate pressure and drawing it across the surface in different directions eight-times.

2.2 CO_2 laser surface treatment arrangement

A 3 kW CO_2 laser (TLC105; Trumpf, Ltd.) emitting at a wavelength of 10.6 μm was used for the surface treatment of the Ti6Al4V alloy. The laser was operated in the continuous wave (CW) mode. The CO_2 laser beam was defocused to a 7 mm spot diameter and operated with a laser power of 1.3 and 1.6 kW. The CO_2 laser beam was traversed across the surface of the Ti6Al4V alloy at a speed of 4800 mm/min. The fumes produced were removed with an extraction system whilst an O_2 assist gas was supplied at 2 bar pressure to shield the CO_2 laser optics.

2.3 Surface characterisation

The surface roughness (measured in terms of R_a) of the untreated, mechanically roughened and CO_2 laser treated Ti6Al4V alloy specimens was measured using a profilometer (Surface Tester SV-600; Mitutoyo, Inc.). Five measurements were made in three different places on each sample and mean values of surface roughness

(given in terms of R_a) were then obtained. X-ray photoemission spectroscopy (XPS) (AXIS Ultra; Kratos, Inc.) was used to characterise the surface oxygen content of the untreated, mechanically roughened and CO_2 laser treated Ti6Al4V alloy samples. The XPS analysis was performed on the surface of the samples using a spectrometer with monochromatic Al Kα (1486.71 eV) X-ray radiation (15 kV and 10 mA) and a hemispherical electron energy analyser.

2.4 Wettability characterisation

To examine the wetting and surface energy characteristics of the Ti6Al4V alloy when in the untreated, mechanically roughened and CO_2 laser treated condition, wetting experiments were conducted. A set of sessile drop control experiments was carried out using glycerol, formamide, etheneglycol, polyglycol E-200 and polyglycol 15–200. The characteristics of the control test liquids are given in previous work [26]. The value of θ for the control test liquids on the untreated mechanically roughened and CO_2 laser treated Ti6Al4V alloy were determined in atmospheric conditions at 25°C using a sessile drop measuring machine (FTÅ 125; First Ten Ångstroms, Inc). Each measurement of θ lasted for three minutes with profile photographs of the sessile drop being obtained every minute and a mean value being subsequently determined. After the control test liquid drops for each liquid attached and rested on the Ti6Al4V alloy surface, the drops consistently reached an equilibrium state in around 6 s. Thereafter they remained motionless and the magnitude of the θ changed little with time. In order to estimate the influence of contaminant layers on the measurement results, the specimens of the untreated Ti6Al4V alloy were cleaned with acetone in an ultrasonic bath for 2 h, rinsed with distilled water several times and dried in a vacuum oven at 90°C for 12 h. All of the five control test liquids were used to measure θ on the cleaned samples. The values of θ on the cleaned samples were lower than on the as-received (not cleaned) samples by 0.8, 0.7, 0.5, 0.3 and 0.2° for glycerol, formamide, etheneglycol, polyglycol E-200 and polyglycol 15–200 respectively. It is therefore reasonable to conclude that the presence of any contaminants on the surface of the Ti6Al4V alloy do not have a great influence on θ. This being the case, the work was conducted in a normal atmospheric environment without pre-cleaning.

2.5 In vitro protein adsorption

The proteins used for this study were human serum albumin and human plasma fibronectin (Calbiochem, Inc.). Prior to the adsorption of 1 mg/ml albumin in phosphate buffered salines (PBS), Ti6Al4V alloy samples were rinsed with deionised water. The individual samples were transferred into a 24-well tissue culture plate. Thereafter, 2.5 ml of prepared albumin solution was added into each well. Adsorption proceeded for 1 h in an incubator at 37 °C. After adsorption was complete, the samples were dried with N_2 and immediately transferred to an ellipsometer for measurement of the adsorbed protein layer. The above procedure was repeated with a 0.2 mg/ml concentration fibronectin in PBS.

2.6 Ellipsometric measurement

The thickness of adsorbed human serum albumin and human plasma fibronectin on the Ti6Al4V were measured using an automatic ellipsometer equipped with a 632.8 nm helium-neon laser (L117F; Gaertner, Inc.). The thickness and refractive indices of protein films were determined using an ellipsometer computer program. Four ellipsometer measurements at different locations on each sample were taken and the average value was calculated.

2.7 Statistics

Statistical analysis was performed with a SPSS v.12 software package (SPSS/PC Inc.). Data are reported as mean ± SD at a significance level of $p < 0.05$. After having verified normal distribution and homogeneity of variances, one-way ANOVA and Scheffé's post hoc multiple comparison tests were done.

3 Results

3.1 Morphological analysis and surface roughness

The typical surface view of the untreated Ti6Al4V alloy, as shown in Fig. 1a, exhibited regularly ordered parallel and longitudinal grooves. From Fig. 1b it can be seen that the mechanically roughened Ti6Al4V alloy samples also presented a grooved surface. But in contrast to the untreated Ti6Al4V alloy surface, the mechanically roughened samples typically displayed no surface ordering: with the grooves being orientated in various directions. The surfaces of both of the CO_2 laser treated Ti6Al4V alloy samples retained a similar morphology to that of the untreated sample insofar as parallel and longitudinal grooves that are regular in size and periodicity are present (see Fig. 1c, d). It

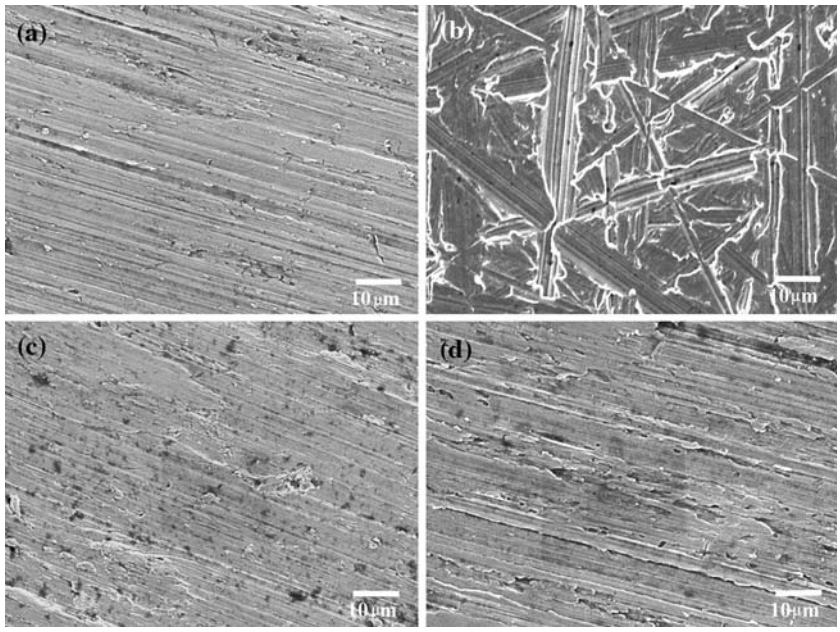

Fig. 1 Typical SEM surface images of the Ti6Al4V alloy (**a**) untreated, (**b**) mechanically roughened and CO_2 laser treated at power densities of (**c**) 1.3 kW/cm^2 and (**d**) 1.6 kW/cm^2

appears that CO_2 laser radiation, when incident with the Ti6Al4V alloy, resulted in partial melting and resolidification. The differing CO_2 laser power densities applied yielded surface melting to varying degrees. In the case of the sample treated at a CO_2 laser power density of 1.6 kW/cm^2, the higher power density used would result in more energy being absorbed thereby causing more surface melting to occur. In contrast, the sample treated at a CO_2 laser power density of 1.3 kW/cm^2 was treated with less power density and so less energy was absorbed. Naturally then, the specimen treated at 1.6 kW/cm^2 experienced a higher degree of melting and resolidification and so the depth of the grooves was much greater (see Fig. 1d), whereas the specimen treated at CO_2 laser power density of 1.3 kW/cm^2 underwent melting and resolidification to a lesser extent and thus the depth of the grooves was shallower (see Fig. 1c). It is worth remarking that since the surface morphologies of the two CO_2 laser treated samples, while being different to the untreated sample, are not dramatically different from each other. Once can therefore assert that the energy absorbed was neither insufficient nor excessive.

From Fig. 2, one can see that the surface of the Ti6Al4V in the untreated condition was reasonably smooth, having an average surface roughness value of 0.35 μm. The average surface roughness value of the Ti6Al4V alloy increased to 0.39 μm when treated with a CO_2 laser power density of 1.3 kW/cm^2, and to 0.42 μm when treated with a CO_2 laser power density of 1.6 kW/cm^2. The mechanical roughening had more

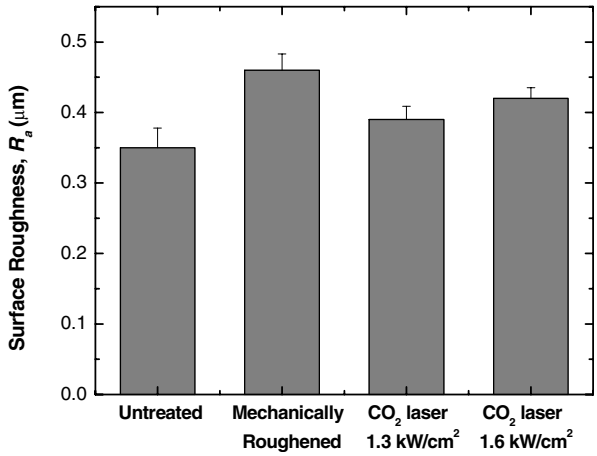

Fig. 2 Mean values of surface roughness for the untreated, mechanically roughened and CO_2 laser treated Ti6Al4V alloy

of a marked effect on surface roughness and resulted in the maximum surface roughness: 0.47 μm.

3.2 Surface oxygen content

From the XPS results given in Fig. 3 one can see that the mechanically roughened sample had a similar value of surface oxygen content to that of the untreated specimen. On the other hand, the surface oxygen content increased in Ti6Al4V alloy after CO_2 laser treatment. Moreover, Fig. 3 reveals that as the CO_2 laser power density was increased from 1.3 to 1.6 kW/cm^2, the surface oxygen content increased further. Similarly Lawrence et al. [27] observed that the surface

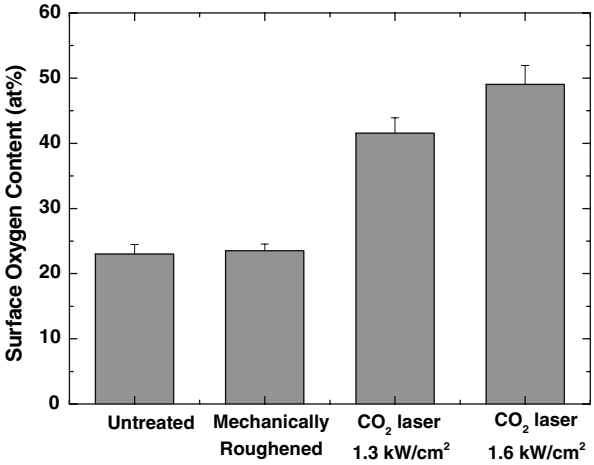

Fig. 3 Mean values of surface oxygen content for the untreated, mechanically roughened and CO_2 laser treated Ti6Al4V alloy

oxygen content of a carbon steel increased after CO_2 laser treatment. Based on the findings of Lawrence et al. [27] it is possible to maintain that the general increase in the surface oxygen of the Ti6Al4V alloy after CO_2 laser treatment was due to the natural occurrence of oxidization during the CO_2 laser surface treatment. Surface oxidation is likely the cause of the observed increase in the surface oxygen content of the Ti6Al4V alloy sample treated with the higher CO_2 laser power density: as the increased CO_2 laser power density would result in higher melting thereby promoting the absorption of more oxygen into Ti6Al4V alloy surface.

3.3 Wettability and surface energy analysis

The mean values of θ for the five control test liquids measured on the untreated, mechanically roughened and CO_2 laser treated Ti6Al4V alloy are given in Table 1. Consideration of the data in Table 1 reveals that mechanical roughening of the surface of the Ti6Al4V alloy occasioned reductions in θ for all of the control test liquids, but it is clear that these reductions were only moderate. In contrast, it can be seen from Table 1 that CO_2 laser treatment of the surface of the Ti6Al4V alloy (at both 1.3 and 1.6 kW/cm^2) resulted in marked decreases in θ with all of the control test liquids, with the greatest reductions in θ occurring when the laser power density was 1.6 kW/cm^2.

Now, the value of θ is related to the solid and liquid surface energies, γ_{sv} and γ_{lv} respectively, and the solid-liquid interfacial energy, γ_{sl}, through the principal of virtual work expressed by Young's equation:

$$\gamma_{sv} = \gamma_{lv}\cos\theta + \gamma_{sl} \tag{1}$$

The adhesion intensity of a liquid to a solid surface is known as the work of adhesion, W_{ad}, and is given by the Young–Dupre equation:

$$W_{ad} = \gamma_{lv}(1 + \cos\theta) \tag{2}$$

The intermolecular attraction which is responsible for total surface energy, γ, results from a variety of intermolecular forces whose contribution to the total surface energy is additive [28]. The majority of these forces are functions of the particular chemical nature of a certain material, and as such the total surface energy comprises of γ^p (polar or non-dispersive interaction) and γ^d (dispersive component: since van der Waals forces are present in all systems regardless of their chemical nature); consequently, γ of any system can be described by [29]

$$\gamma = \gamma^d + \gamma^p \tag{3}$$

Similarly, W_{ad} can be expressed as the sum of the different intermolecular forces that act at the interface [30]:

$$W_{ad} = W_{ad}^d + W_{ad}^p = 2\left(\gamma_{sv}^d\gamma_{lv}^d\right)^{1/2} + 2\left(\gamma_{sv}^p\gamma_{lv}^p\right)^{1/2} \tag{4}$$

Table 1 Measured contact angle values for the untreated, mechanically roughened and CO_2 laser treated Ti6Al4V alloy

Control Test Liquid	Contact Angle, θ (deg)			
	Untreated	Mechanically roughened	CO_2 Laser Treated (kW/cm^2)	
			1.3	1.6
Glycerol	85.8	78.7	74.4	70.1
Formamide	83.6	74.5	72.6	67.6
Etheneglycol	77.3	70.9	68.4	62.9
Polyglycol E-200	71.1	64.5	63.2	57.3
Polyglycolycol 15–200	67.1	55.3	53.5	48.1

By equating Eq. 4 with Eq. 2, the value of θ for solid-liquid systems where both dispersion forces and polar forces are present can be related to the surface energies of the respective liquid and solid by

$$\cos\theta = \frac{2\left(\gamma_{sv}^{d}\gamma_{lv}^{d}\right)^{1/2}+2\left(\gamma_{sv}^{p}\gamma_{lv}^{p}\right)^{1/2}}{\gamma_{lv}} - 1 \quad (5)$$

where γ_{sv}^{p} and γ_{sv}^{d} are the dispersive component and polar components respectively of the solid surface energy, γ_{sv}.

As has already been detailed in a previous study by Hao and Lawrence [26], it is possible to estimate reasonably accurately the γ_{sv}^{d} of the Ti6Al4V alloy by plotting the graph of cos θ against $(\gamma_{lv}^{d})^{1/2}/\gamma_{lv})$ in accordance with Eq. 5. Figure 4 shows the best-fit plot of cos θ against $(\gamma_{lv}^{d})^{1/2}/\gamma_{lv})$ for the untreated, mechanically roughened and CO_2 laser treated Ti6Al4V alloy-experimental control liquids system. Thereafter it is possible to calculate γ_{sv}^{p} from the value of γ_{sv}^{d}. It is not possible to determine the value of γ_{sv}^{p} for the Ti6Al4V alloy directly, but the following can be derived:

$$\left(\gamma_{sv}^{p}\right)^{1/2} = \frac{\left(\gamma_{sv}^{d}\right)^{1/2}(a-1)}{c} \quad (6)$$

where a can be determined from the best-fit line of W_{ad} (Work adhesion) against W_{ad}^{d}(dispersive component of work adhesion) of the Ti6Al4V alloy [24], while c can be deduced from the best-fit line of γ_{lv}^{p} and γ_{lv}^{d} of the test liquids as described in previous work [26]. Thus, from the best-fit straight line plots of W_{ad} against it is possible to determine the constant, a, for each separate condition of the Ti6Al4V alloy: 2.38 in the untreated condition; 2.66 when mechanically roughened; 2.80 when CO_2 laser treated at 1.3 kW/cm^2 and 2.84 when CO_2 laser treated at 1.6 kW/cm^2. Similarly, from a linear relationship existing between the of γ_{lv}^{p} and γ_{lv}^{d} of the control liquids, the constant, c, is determined to be 2.9. It is therefore possible to calculate γ_{sv}^{p} directly for the untreated, mechanically roughened and CO_2 laser treated Ti6Al4V alloy using Eq. 6 with the determined values of the constants, a, and, c. As is evident from Fig. 5, both mechanical roughening CO_2 laser treatment of the surface of the Ti6Al4V alloy led to an increase in the total surface energy. But, perhaps of more importance, the CO_2 laser treatment brought about a considerable increase in the value of γ_{sv}^{p} for the Ti6Al4V alloy; such a marked increase in γ_{sv}^{p} was not observed for the mechanically roughened sample.

3.4 Investigation of wettability and work of adhesion using physiological liquids

In order to simulate the biological environment, physiological fluids and simulated physiological liquids were used for additional wetting experiments. The biological liquids selected were human blood, human blood plasma, simulated body fluid (SBF) and SBF + BSA (bovine serum albumin). The SBF was prepared by dissolving reagent-grade chemicals, NaCl, $NaHCO_3$, KCl, $K_2HPO_4.3H_2O$, $MgCl_2.6H_2O$, $CaCl_2$ and Na_2SO_4 in ion-exchanged and distilled water, buffered at pH 7.25 at 37°C with tris(hydroxymethyl) aminomethane ($[CH_2OH]3CNH_2$) and 1 m hydrochloric acid (HCl). The SBF has an inorganic ion concentration close to that found in human blood plasma.

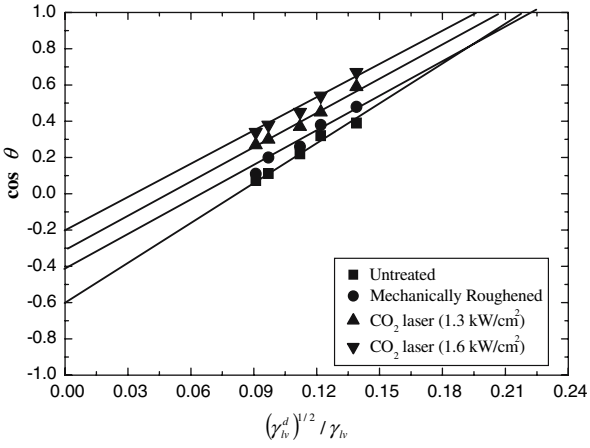

Fig. 4 Plot of cos θ against $(\gamma_{lv}^{d})^{1/2}/\gamma_{lv}$ for the untreated, mechanically roughened and CO_2 laser treated Ti6Al4V alloy in contact with the control test liquids

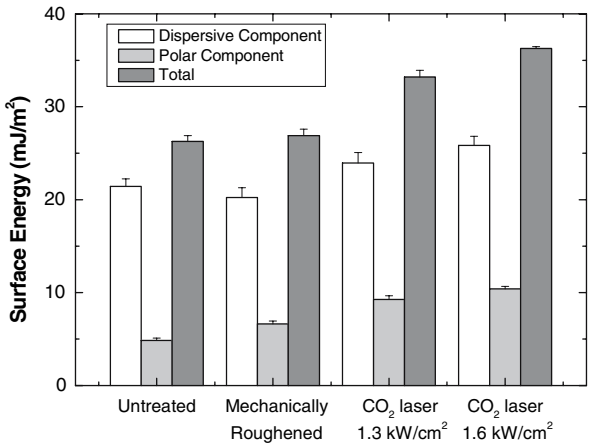

Fig. 5 Measured total surface energy (γ_{sv}), dispersive (γ_{sv}^{d}) and polar (γ_{sv}^{p}) components for the untreated, mechanically roughened and CO_2 laser treated Ti6Al4V alloy

Table 2 Mean values of contact angles formed between the physiological test liquids and the untreated, mechanically roughened and CO_2 laser treated Ti6Al4V alloy

Ti6Al4V alloy	Contact angle, θ (deg)			
	Human blood	Human blood plasma	SBF	SBF + BSA
Untreated	58.3	63.2	82.8	60.9
Mechanically roughened	56.9	61.7	80.2	59.1
CO_2 Laser (1.3 kW/cm^2)	50.6	55.4	71.0	53.5
CO_2 Laser (1.6 kW/cm^2)	48.3	53.6	68.2	51.2

SBF + BSA was prepared using bovine serum albumin (BSA) (Sigma A-9306; lot number 106H0300) dissolved in SBF at pH 7.25 with a concentration of 4 mg/ml, to be used for protein studies to simulate human albumin because it is very similar to the sequence of amino acid units.

The values of θ formed between the selected and simulated physiological test liquids and the untreated, mechanically roughened and CO_2 laser treated Ti6Al4V alloy sample are given in Table 2. Table 2 shows clearly that the values of θ for all the body fluids on the CO_2 laser treated Ti6Al4V alloy are lower than on the untreated and mechanically roughened specimens, indicating that the wettability of the material with the body fluids improved significantly after CO_2 laser treatment. Further, according to the Eq. 4, the decrease in the value of θ resulted naturally in an increase in W_{ad} of the Ti6Al4V towards to the physiological and simulated physiological liquids. Using the referenced values for γ_{lv} for the selected biological liquids: human blood (47.5 mJ/m^2), human blood plasma (50.5 mJ/m^2) [31], SBF (72.5 mJ/m^2) and SBF + BSA (54.0 mJ/m^2) [32] W_{ad} values for the Ti6Al4V alloy towards these body fluids were determined and are given in Fig. 6. A discernable increase in the W_{ad} of the selected body fluids on the Ti6Al4V alloy following CO_2 laser treatment is apparent from Fig. 6; moreover, W_{ad} increased as the CO_2 laser power density increased.

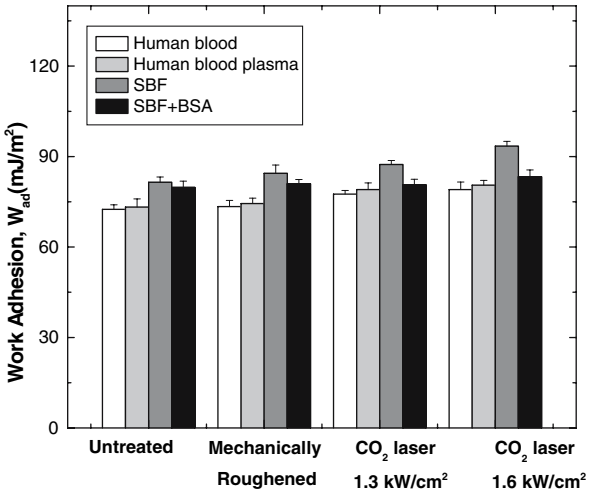

Fig. 6 Work of adhesion of body fluids for the untreated, mechanically roughened and CO_2 laser treated Ti6Al4V alloy

3.5 Protein adsorption analysis

The thickness of the adsorbed albumin and fibronectin layers in vitro on the untreated and CO_2 laser modified Ti6Al4V alloy—which would be an indication of the amount of adsorbed protein on the untreated and CO_2 laser modified Ti6Al4V alloy—are shown in the Fig. 7. It was found that the thickness of the albumin layer on the untreated Ti6Al4V alloy sample was higher than that on the CO_2 laser modified sample. In contrast, the thickness of the fibronectin layer was less on the untreated Ti6Al4V alloy sample than that on the modified sample. So, it is possible to assert that the CO_2 laser power density applied in the experiment is negatively correlated to the albumin adsorption, whilst being positively correlated with the fibronectin adsorption.

4 Discussion

4.1 CO_2 laser-induced enhancement of wettability characteristics of the Ti6Al4V alloy

An increase in the wettability of the Ti6Al4V alloy could be generated either mechanically roughening or CO_2 laser treating its surface. But compared with mechanical roughening, CO_2 laser treatment resulted in greater decreases in the value of θ and was therefore more effective in modifying the wettability of the Ti6Al4V alloy. Moreover, the value of θ was seen to decrease as the CO_2 laser power density increased, showing that the wettability of the Ti6Al4V alloy was influenced by the laser processing parameters and could consequently be controlled. The results detailed

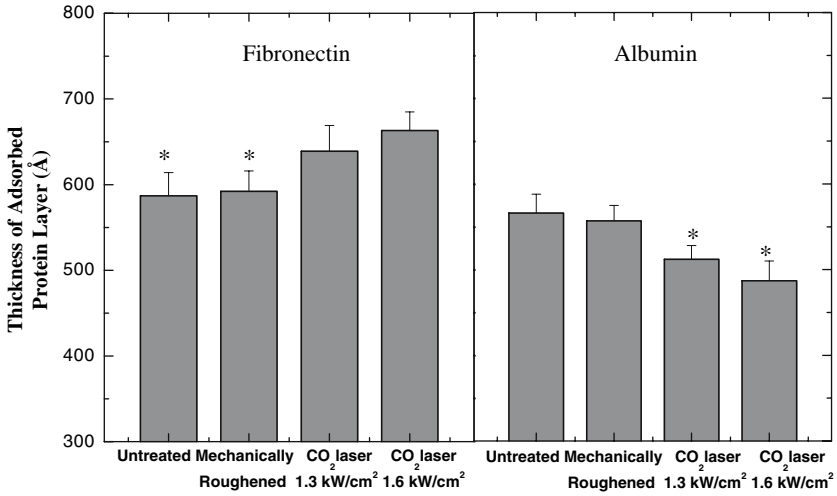

Fig. 7 Thickness of the adsorbed fibronectin and albumin protein layer on the untreated and CO_2 laser treated Ti6Al4V alloy (treated with different power densities). (For both fibronectin and albumin adsorption, there was significant statistical difference in thickness between the untreated Ti6Al4V alloy and the samples CO_2 laser treated at 1.3 and 1.6 kW/cm^2, and no statistical difference between the untreated and the mechanically roughened Ti6Al4V alloy. $^*p < 0.05$)

above suggest that modification of the surface roughness, surface oxygen content and surface energy of the Ti6Al4V alloy were the factors governing the observed changes in the wettability.

A model similar to that for heterogeneous solid surfaces can be developed in order to account for surface irregularities, being given by Wenzel's equation [33]:

$$r_\alpha(\gamma_{sv} - \gamma_{sl}) = \gamma_{lv}\cos\theta_W \tag{7}$$

where r_α is the roughness factor defined as the ratio of the true to apparent surface areas and θ_W is the contact angle for the wetting of a rough surface. If r_a is large, that is the surface is rough, then $\cos\theta_W$ is large and θ_W will decrease if θ was originally less than 90°. So, when r_a increases θ_W decreases if θ was originally less than 90°. In the instance when θ is originally greater than 90°, then the situation is vice versa.

In the case of the mechanically roughened samples, the value of the surface oxygen content and the γ_{sv}^p remained virtually the same as those prior to the roughening process (see Table 1). Consequently it is reasonable to assume that the decrease in θ caused by the mechanical roughening was due solely to the increase in surface roughness in accord with Eq. 7. Significantly, Figs. 3 and 5 shows that the surface oxygen content and the value of γ_{sv}^p of the sample subjected to mechanical roughening remained virtually the same as the untreated sample, thus indicating that the decrease in θ and the increase in surface roughness alone caused the wettability characteristics to increase. But a review of the results given Sect. 3.3 and 3.4 show CO_2 laser treatment is more effective in enhancing the wettability characteristics of the Ti6Al4V alloy, in spite of the fact that mechanical roughening generated a rougher surface. This would suggest that the changes in the other surface properties associated with the CO_2 laser treatment (surface oxygen content and surface energy, which are modified simultaneously) play a significant role in modifying the wettability characteristics of the Ti6Al4V alloy. By extension then, the increase in surface roughness caused by mechanically roughening and CO_2 laser treatment contributes to the increase of wettability. As for stainless steel, surface roughness was identified as the predominant factor governing the change of wettability after laser treatment [34].

For CO_2 laser treatment, it generated the changes in surface oxygen content and surface energy that could influence the wettability. This is why although the mechanical roughening resulted in the roughest surface, its effect on θ was less that of CO_2 laser treatment. The higher level of surface oxygen content is corresponding to the higher wettability. This is believed to be due to the oxidisation of the Ti6Al4V surface during melting, indicating that oxygen enrichment of the Ti6Al4V surface is active in promoting wetting and adhesion, as well as bonding. In fact, the surface oxygen content was found to a factor contributing the wettability enhancement of a carbon steel following the surface treatment by a high power diode laser [35] and a 316 LS stainless steel bio-metal following the surface treatment by a Nd:YAG laser

[36] and high power diode laser [24]. Hence, the wetting performance of the Ti6Al4V would have certainly been influenced by the increase in the oxygen content of the Ti6Al4V surface as a result of the laser treatment, since this is known to increase the likelihood of wetting [37, 38].

The increase of γ_{sv} and γ_{sv}^{p} surface energy of Ti6Al4V is corresponding to the improvement of wettability and plays as another influencing factor. Enhancement of surface energy is thought to be due to the fact that CO_2 laser treatment results in the melting and resolidification of Ti6Al4V alloy surface, a transition that is known to effect an increase in γ_{sv}^{p} [39–41], and thus improvement in the wettability and an increase in the adhesion at the interface in contact with the test liquids. This explains why after laser treatment, specimens have better wettability. The higher power density yielded higher extent of surface melting on Ti6Al4V and thereby resulted in higher value of γ_{sv}^{p}. Hence, the increase of γ_{sv}^{p} is believed to be the predominant mechanism governing the change in wettability of Ti6Al4V following laser irradiation. Indeed, it has been identified that the surface energy, especially γ_{sv}^{p}, presented by the laser rapid solidified microstructure after surface melting, was the major factor influencing the wettability of the CO_2 laser treated MgO-PSZ [42] and yttria partially stabilised zirconia [43], the high power diode laser treated alumina bioceramic [44] and the modified steel by various lasers [35, 45].

From this one can see that the increase in wettability was created by the CO_2 laser modification of surface roughness, surface oxygen content and surface energy. The CO_2 laser treatment effected a higher wettability than the mechanically roughness due to the fact that CO_2 laser surface generated three influencing factors simultaneously while mechanical roughening just changed one influencing factor.

4.2 The effects of CO_2 laser treatment on the interactions of physiological liquids and proteins with the Ti6Al4V alloy

The lower θ formed between the physiological liquids and CO_2 laser treated Ti6Al4V alloy surface imply that the interaction of the Ti6Al4V alloy with body fluids might be improved owing to the improved wettability. Since biomaterials first contact a proteinaceous liquid phase, almost aqueous in nature, leading to surface reorganization of proteins followed by cell attachment on biomaterials, wettability, by controlling the interaction with physiological fluids, would primarily influence cell behaviour on biomaterials. Wetting of the solid surface is a typical predictive index of cytocompatibility [46]. Moreover, the improvements of W_{ad} towards these fluids would imply better suitability of titanium alloy in biological environment.

CO_2 laser treatment caused a considerable difference in the amount of in vitro protein adsorption on the Ti6Al4V alloy surface. As one can see from Fig. 7, on the one hand the CO_2 surface treatment promoted the adsorption of the fibronectin and the amount of the adsorbed fibronectin on the Ti6Al4V alloy surface was positively correlated with the CO_2 laser power; on the other hand it inhibited the albumin adsorption and the amount of the adsorbed albumin was negatively correlated with CO_2 laser power. It is known that protein adsorption is influenced by the surface chemistry (wettability) [47] and the surface topography [48]. The study by Deligianni et al. [49] showed that a rougher Ti6Al4V alloy surface prepared by polishing occasioned less albumin adsorption and higher fibronectin adsorption. This also was the case for the mechanically roughened sample in this study where less albumin adsorption and higher fibronectin adsorption compared with the untreated sample was observed; however, the difference between these samples is not statistically significant. Although CO_2 laser treatment did not generate the roughest surface, the samples following CO_2 laser treatment exhibited a statistically significant difference in protein adsorption from the untreated sample. Hence, a clear conclusion could not be made for the effect of surface roughness.

A clear relationship between the albumin and fibronectin adsorption wettability of the Ti6Al4V was observed in Fig. 8. The albumin decreases with increasing wettability. The results of the albumin adsorption are consistent with the previous finding

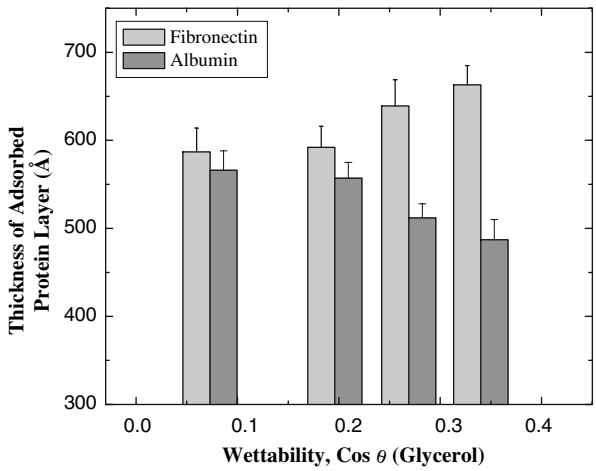

Fig. 8 The relationship between the thickness of the adsorbed fibronectin layer and wettability (cos θ) of the Ti6Al4V alloy

that the increase in surface hydrophilicity of Ti results in lower albumin adsorption [50], showing that the wettability of the Ti6Al4V could be the factor active in the albumin adsorption. Moreover, previous studies revealed that albumin absorption decreased on CO_2 laser treated MgO-PSZ [20] due to the increased wettability. On the other hand, the adsorption of fibronectin increases with the increasingly wettable characteristics (hydrophilic) Ti6Al4V surface, implying that wettability is the predominant mechanism governing the fibronectin adsorption. A previous investigation [51] on the extent of fibronectin adsorption as compared to its biological activity on hydrophobic and hydrophilic surfaces suggested the possibility that fibronectin was adsorbed in two different conformations when incubated with the surfaces a low concentrations, with the more active conformation on the hydrophilic surfaces. The results showed the anti-plasma fibronectin antibody appeared to bind to the conformation of fibronectin adsorbed on hydrophilic surfaces much better than the conformation of fibronectin adsorbed on hydrophobic surfaces [51]. It is noticeable that considerable change in the γ_{sv}^{p} instead of minor difference in γ_{sv}^{d} (see Fig. 5) was the main mechanism governing the wettability after CO_2 laser irradiation, indicating that the albumin and fibronectin adsorption on the Ti6Al4V surfaces was probably due to the polar and chemical interactions [52]. This finding is similar to the previous investigation that albumin and fibronectin adsorption is mainly influenced by the change in $\gamma_{sv}^{p}$of the MgO-PSZ following CO_2 laser irradiation [20]. It is therefore possible to maintain that the change in $\gamma_{sv}^{p}$of the Ti6Al4V alloy—effected by the CO_2 laser irradiation—contributes to the inhabitation of albumin adsorption and the enhancement of fibronectin adsorption thereby increasing the potential for favourable bone cell response on the Ti6Al4V.

5 Conclusions

Modification of the surface properties of a Ti6Al4V alloy was achieved using a CO_2 laser. This in turn brought about an increase in the propensity of the Ti6Al4V alloy to wet and increased the adsorption of human plasma fibronectin but decreased the adsorption of human serum albumin. The improvements in the wettability of the Ti6Al4V alloy following CO_2 laser treatment were identified as being due mainly to the increase in surface roughness, surface oxygen content and surface energy of the material. When compared with untreated and mechanically roughened samples CO_2 laser treated samples exhibited lower amounts of adsorbed albumin and higher amounts of adsorbed fibronectin. As the wettability of the Ti6Al4V alloy increased the adsorbed amounts of fibronectin increased, while the adsorbed amounts of albumin decreased—indicating the controllability of the CO_2 laser process. Such an observation would suggest that the wettability of the Ti6Al4V alloy was the prime influence on the observed changes in in vitro protein adsorption. Further, the noted considerable change in the polar component of surface energy, γ_{sv}^{p}, on the protein adsorption implied that the protein adsorption on the Ti6Al4V alloy was probably due to the polar and chemical interactions. This work has demonstrated that CO_2 laser radiation could be a suitable means to modify the wettability of the Ti6Al4V alloy and thereby manipulate protein adsorption and consequently render the material more bone cell responsive.

References

1. F. J. GIL, A. PADROS, J. M. MANERO, C. APARICIO, M. NILSSON and J. A. PLANELL, *Mater. Sci. Eng. C* **22** (2002) 53.
2. W. NORDE, *Adv. Colloid Interface Sci.* **25** (1986) 267.
3. C. A. HAYNES and W. NORDE, *Colloids Surf. B: Biointerfaces* **2** (1994) 517.
4. W. NORDE, *Cells Mater.* **5** (1995) 97.
5. F. GRINNELL, *Inter. Rev. Ctyol.* **53** (1978) 65.
6. T. A. HORBETT and M. B. SCHWAY, *J. Biomed. Mater. Res.* **22** (1988) 763.
7. A. DEKKER, K. REITSMA, T. BEUGELING, A. BANTJES, J. FEIJEN and W. G. Van AKEN, *Biomaterials* **12** (1991) 130.
8. J. K. SMETANA, *Biomaterials* **14** (1993) 1046.
9. B. D. BOYAN, T. W. HUMMERT, D. D. DEAN and Z. SCHWARTZ, *Biomaterials* **17** (1996) 137.
10. J. M. SCHAKENRAAD, H. J. BUSSCHER, C. R. H. WILDEVUUR and J. ARENDS, *J. Biomed. Mater. Res.* **20** (1986) 773.
11. P. B. Van WACHEM, T. BEUGELING, J. FEIJEN, A. BANTJES, J. P. DETMERS and W. G. Van AKEN, *Biomaterials* **6** (1985) 403.
12. Y. TAMADA and Y. IKADA, *Polymer* **34** (1993) 2208.
13. C. C. ANNARELLI, J. FORNAZERO, R. COHEN, J. BERT and J. L. BESSE, *J. Colloid Interface Sci.* 213 (1999) 386.
14. A. G. GRISTINA, *Science* **237** (1987) 1588.
15. H. MIRZADEH, A. A. KATBAB and R. P. BURFORD, *Radiation Phys. Chem.* **46** (1995) 859.
16. H. MIRZADEH, A. A. KATBAB, M. T. KHORASANI, R. P. BURFORD, E. GORGIN and A. GOLESTANI, *Biomaterials* **16** (1995) 641.
17. M. DADSETAN, H. MIRZADEH, N. SHARIFI-SANJANI and M. DALIRI, *J. Biomed. Mater. Res.* 57 (2001) 183.
18. L. HAO, J. LAWRENCE, D. K. Y. LOW, K. S. CHIAN, G. C. LIM and H. Y. ZHENG, *J. Mater. Sci. Mater. Med.* **15** (2004) 967–975.

19. L. HAO and J. LAWRENCE, *Colloids Surf. B: Biointerfaces* **34** (2004) 87.
20. L. HAO and J. LAWRENCE, *J. Biomed. Mater. Res.* **69A** (2004) 748.
21. L. HAO and J. LAWRENCE, *Mater. Sci. Eng. C* **23** (2003) 627.
22. L. HAO, J. LAWRENCE and K. S. CHIAN, *J. Biomaterials Appl.* **19** (2004) 81.
23. L. Hao, D. R. Ma, J. Lawrence, Z. X. Mater. *Sci. Eng. C: Biomimetic and Supramolecular Systems*, In press (2005).
24. L. HAO, J. LAWRENCE and L. LI, *Appl. Surf. Sci.* **247** (2005) 453.
25. L. HAO, J. LAWRENCE and L. LI, *Appl. Surf. Sci.* **247** (2005) 602.
26. L. HAO and J. LAWRENCE, *J. Phys. D Appl. Phys.* **36** (2003) 1292.
27. J. LAWRENCE, L. LI, *Appl. Surf. Sci.* **154–155** (2000) 664.
28. N. K. ADAM, G. E. P. ELLIOTT, *J. Chem. Soc.* **18** (1958) 2206.
29. F. M. FOWKES, *Ind. Eng. Chem.* **56** (1964) 40.
30. J. R. DANN, *J. Colloid Interface Sci.* **32** (1970) 302.
31. S. AGATHOPOULOS and P. NIKOLOPOULOS, *J. Biomed. Mater. Res.* **29** (1995) 421.
32. M. AMARAL, M. A. LOPES, J. D. SANTOS and R. F. SILVA, *Biomaterials*, **23** (2002) 4123.
33. R. N. WENZEL, *Ind. Eng. Chem.* **28** (1936) 988.
34. J. LAWRENCE and L. LI, *J. Laser Appl.* **14** (2002) 107.
35. J. LAWRENCE and L. LI, *Optics Lasers Eng.* **32** (1999) 353.
36. J. LAWRENCE, H. R. CHEW, C. K. CHONG and L. HAO, *Lasers Eng.* **15** (2005) 75.
37. Q. SONG and A. N. NETRAVALI, *J. Adhesion Sci. Tech.* **12** (1998) 957.
38. J. LAWRENCE and L. LI, Laser modification of the wettability characteristics of engineering materials, Professional Engineering: London (2001).
39. R. J. GOOD and L. A. GIRIFALCO, *J. Phys. Chem.* **64** (1960) 561.
40. J. LAWRENCE, L. LI and J. T. SPENCER, *Appl. Surf. Sci.* **138–139** (1999) 388.
41. J. LAWRENCE and L. LI, *J. Phys. D* **32** (1999) 1075.
42. L. HAO and J. LAWRENCE, *J. Laser Appl.* **16** (2004) 252.
43. L. HAO, J. LAWRENCE and K. S. CHIAN *J. Mater. Sci. Mater. Med.* **16** (2005) 719.
44. J. LAWRENCE, *Pro. Roy. Soc. A Math. Phys. Eng. Sci.* **460** (2004) 1723.
45. J. LAWRENCE and L. LI, *Phys. D* **32** (1999) 2311.
46. M. LAMPIN, R. WAROCQUIER-CLEROUT, C. LEGRIS, M. DEGRANGE and M. F. SIGOT-LUIZARD, *J. Biomed. Mater. Res.* **36** (1997) 99.
47. J. OLSSON, A. CARLEN, N. L. BURNS and K. HOLMBERG, *Colloids Surf. B Biointerfaces* **5** (1995) 161.
48. C. GALLI, M. COLLAUD COEN, R. HAUERT, V. L. KATANAEV, P. GRONING and L. SCHLAPBACH, *Colloids Surf. B Biointerfaces* **26** (2002) 255.
49. D. D. DELIGIANNI, N. KATSALA, S. LADAS, D. SOTIROPOULOU, J. AMEDEE and Y. F. MISSIRLIS, *Biomaterials,* **22** (2001) 1241.
50. A. P. SERRO, A. C. FERNANDES, B. SARAMAGO and W. NORDE, *J. Biomed. Mater. Res.* **46** (1999) 376.
51. F. GRINNELL and M. K. FELD, *J. Biological Chem.* **257** (1982) 4888.
52. B. FENG, J. WENG, B. C. YANG, J. Y. CHEN, J. Z. ZHAO, L. HE, S. K. QI and X. D. ZHANG, *Mater. Characterization* **49** (2002) 129.